ISODRIP, a model to transfer the $\delta^{18}O$ signal of precipitation to drip water — implementation of the model for Eagle Cave (central Spain)

Domínguez-Villar, David; Krklec, Kristina; Boomer, Ian; Fairchild, Ian J.

DOI:
10.1016/j.scitotenv.2021.149188

ISODRIP, a model to transfer the $\delta^{18}O$ signal of precipitation to drip water — Implementation of the model for Eagle Cave (central Spain)

David Domínguez-Villar[1]*, Kristina Krklec [1], Ian Boomer[2], Ian J. Fairchild[2]

[1] Department of Soil Science, Faculty of Agriculture, University of Zagreb, Svetošimunska 25, 10000, Zagreb, Croatia

[2] School of Geography, Earth and Environmental Sciences, University of Birmingham, Edgbaston, Birmingham B15 2TT, United Kingdom

ABSTRACT

The isotope signature of cave waters provides an excellent opportunity to better understand the recharge in karst regions and the complexity of drainage systems in the vadose zone. We have developed a cave isotope hydrological model (ISODRIP) that requires entering basic hydrometeorological information and a precipitation $\delta^{18}O$ record to simulate the discharge and $\delta^{18}O$ signals of different drip sites. The model includes four different modules to simulate various flow route regimes: continuous and discontinuous drips under diffuse or preferential flows. We use precipitation and cave water $\delta^{18}O$ records that were obtained in Eagle Cave (central Spain) during a 5-year period to test our model and to better understand the dynamics of karst aquifers. Eagle Cave waters do not record evaporation. The $\delta^{18}O$ signals do not have seasonality, although they record intra-annual and inter-annual variability. Additionally, cave water $\delta^{18}O$ signal falls within the range of the annual average weighted isotope composition of precipitation. Well-mixed cave waters, that characterize diffuse flows, record 1‰ $\delta^{18}O$ variability, whereas partially-mixed waters, that flow along preferential drainage routes, have up to 3‰ $\delta^{18}O$ variability. The results suggest that precipitation takes on average 15 months to reach the cave through the diffuse flow network, whereas under preferential flow the transit time is highly variable depending on the previous condition of the system. ISODRIP includes a soil layer above the vadose zone that controls large recharge events, together with direct recharge components that bypass the soil layer enabling at least some recharge all year round. Thus, the simulations reproduce the observed lack of seasonal bias in the cave water $\delta^{18}O$ composition in relation to the average weighted isotope composition of precipitation. This research highlights the importance of understanding recharge dynamics and the configuration of particular drips sites to properly interpret speleothem $\delta^{18}O$ records.

Keywords: Transfer function; Simulation; Oxygen isotopes; Cave drip water; Karst hydrology

*Corresponding author at Department of Soil Science, Faculty of Agriculture, University of Zagreb, Zagreb, Croatia. D. Domínguez-Villar, *E-mail address*: ddvillar@hotmail.com

1. Introduction

Signals of climate and environmental conditions that take place over caves are transferred underground, propagated through the bedrock which acts as a filter, and eventually recorded in caves (Fairchild and Baker, 2012). During the transfer process through the vadose zone, the external signal is often smoothed and delayed. The signal transfer depends on several characteristics of the local cave and karst features, but also on the heat or mass transfer processes involved. Thus, a climate or environmental change over a cave that would affect multiple signals (e.g., temperature, amount of precipitation, content of soil CO_2, etc.) may be recorded in the same gallery of the cave at different times, depending on the process that controls the transfer. For example, temperature away from the cave entrances is often controlled by conduction, and climate changes can take from years to millennia depending on the period of the anomaly and the thickness of bedrock over the cave (Moore and Sullivan 1978; Villar et al., 1983; Domínguez-Villar et al., 2015, 2020). On the other hand, air transported underground is frequently dominated by advection, causing a delay of the signal in relation to the surface to be negligible at geological timescales (e.g., Pflitsch et al., 2010; Liñán et al., 2018). In drip waters, the mass transport is affected by both, advective and diffuse transfer processes (Fitts, 2012), and the nature of each flow route imprints singular properties to each drip site (Baker and Fairchild, 2012), affecting the degree of water mixing and the residence time in the vadose zone of karst.

Water isotopes have been traditionally used as tracers to investigate the process of transferring precipitation into caves to better understand underground water flow in the vadose zone of karst regions. Early studies found that in most cases, drip water $\delta^{18}O$

values recorded little variability and their average values were close the annual weighted averages of the $\delta^{18}O$ values of precipitation over the caves (Goede et al., 1982; Yonge et al., 1985). Note that the annual weighted average of precipitation multiplies every monthly isotope value by the monthly amount of precipitation, and the sum of those results during the twelve months of the year is divided by the annual precipitation. Thus, the annual weighted isotope composition of precipitation keeps the mass balance. The lack of seasonality in drip water $\delta^{18}O$ signals indicates the mixing of precipitation within the karst and is often used to suggest residence times of the water of at least one year (Ayalon et al., 1998; Fuller et al., 2008; Pape, 2010; Duan et al., 2016). Conversely, the seasonality in drip water $\delta^{18}O$ signals is often used as evidence for residence times shorter than a year (Carrasco et al., 2006; Partin et al., 2012; Breitenbach et al., 2015; Pérez-Mejías et al., 2018). However, even when drip waters record isotope seasonality, those waters are affected by substantial mixing with previous water in the vadose zone, attenuating the amplitude of the annual cycle (Arbel et al., 2010). In addition, the residence time of water in the soil on top of the bedrock can already last several months (Comas-Bru et al., 2015). Studies that have dated drip waters from different cave systems using tritium isotopes have confirmed that the ages of most drip waters range from less than two years to several decades (Even et al., 1986; Chapman, et al., 1992; Kaufmann et al., 2003; Yamada et al., 2008; Kluge et al., 2010; Jean-Baptiste et al., 2019). Tritium-dated waters that are less than one year old have shown no clear seasonality in the drip water $\delta^{18}O$ signal as a result of mixing with previous waters (Even et al., 1986), confirming the importance of water mixing even in the case of dominant preferential flow drip sites. Furthermore, drip water $\delta^{18}O$ seasonality can result from seasonal mixing of underground water reservoirs of different isotopic composition, regardless their residence time (Bradley et al., 2010), an effect also recorded in other proxies such as fluorescence

(Domínguez-Villar et al., 2018). Therefore, assessments of residence times based on the structure of the drip water $\delta^{18}O$ signal alone should be taken with caution, since they do not consider the full complexity of the karst hydrology.

In the last decade, drip water isotope models have helped to understand not only the residence time but also the flow paths of water in the vadose zone of karst terrains above particular drip sites (Baker et al., 2010; Wackerbarth et al., 2010). The complexity of models differs greatly, ranging from simple weighting and mixing calculations to more complex functions that include evapotranspiration and different flow routes (Baker and Bradley, 2009; Wackerbarth et al., 2010; Bradley et al., 2010; Partin et al., 2012; Baker et al., 2012; Treble et al., 2013; Genty et al., 2014; Moerman et al., 2014; Mischel et al., 2015; Markowska et al., 2016; Domínguez-Villar et al., 2018; Jean-Baptiste, et al., 2019). Isotope hydrology models are especially useful in caves where evaporation impact in drip water is negligible. However, in cave systems with low relative humidity (i.e., <<100%), evaporation causes significant isotope fractionation (Bar Matthews et al., 1996; Ayalon et al., 1998; Cuthbert et al., 2014), which is a major control on the drip water $\delta^{18}O$ signal in addition to the precipitation isotope composition. Furthermore, drip water isotope models are very sensitive to periods of water recharge. During periods of severe water deficit, precipitation events may not contribute to the water isotope composition of the deeper sections of those soils. Consequently, the isotope signature of some rainwater events may not be transferred to the vadose zone during recharge events, eventually modifying the weighted average isotope composition of recharge water compared to precipitation. Although precipitation from every month of the year is often required to reproduce the $\delta^{18}O$ signal of drip waters (e.g., Genty et al., 2014), other cave systems seem to record a biased $\delta^{18}O$ signal compared to the weighted average annual $\delta^{18}O$ value of precipitation, because some rain events during the drier portion of the year do not contribute to the drip water $\delta^{18}O$ signal (e.g., Baker et al., 2019). However, soil isotope studies have shown that regardless of recharge being limited to certain events during the year, the isotope composition at the base of the soil, which accounts for most of the recharge, often has an isotope composition that requires contribution of precipitation from all year round (Gehrels et al., 1998; Comas-Bru et al., 2015). In addition, up to now no drip water isotope model with soil layer has accounted for direct recharge: a component of the recharge that by-passes the soil, entering directly to the vadose zone and that is not affected by evapotranspiration.

Here we present precipitation and cave water $\delta^{18}O$ records obtained during a 5-year monitoring program in Eagle Cave, a small touristic cavern located in central Spain. Using these isotope records in conjunction with meteorological data and information on the drip hydrology, we developed a transfer function that propagates the $\delta^{18}O$ signal of precipitation to various drip sites. This function is a lumped isotope model (named ISODRIP) where precipitation enters the vadose zone trough a soil reservoir as well as direct recharge by-passing the soil reservoir.

2. Study site

Our study site, Eagle Cave, is located in the south of Ávila province in central Spain (40º9’15”N, 5º4’20”W). The cave is formed in a small hill 427 m above sea level that is composed of dolomite and magnesite (Krklec et al., 2016). The cave has a main hall with small passages beside, one of them serving as the entrance (Fig. 1A). The thickness of bedrock over the cave is on average 16 m, being as thin as 8 m in some sectors over the main hall and as thick as 22 m towards the edges of the hall and most lateral galleries

(Domínguez-Villar et al., 2013). A meteorological station operates outside Eagle Cave since 2009, together with a system to collect accumulated precipitation samples at monthly intervals for water stable isotope analyses (Krklec and Domínguez-Villar, 2014). During the period 2009-2013 the mean annual temperature above the cave was 14.7 ºC, the average amount of annual precipitation was 765 mm and the average annual potential evapotranspiration (PET) according to Thornthwaite calculations (Thornthwaite, 1948) is 1163 mm. Freezing events in winter are short-lived and they do not freeze the soil (Krklec et al., 2016). Snow and hail precipitation are rare at the studied site, so, rainwater is the usual form of precipitation. Precipitation has a strong seasonality as expected from a Mediterranean climate such as the one recorded at our study site, and PET is higher than precipitation during 5 months per year: from May to September (Fig. 1B). The vegetation above the cave consists of a typical Mediterranean forest with evergreen oaks and a dense shrubs canopy. In the hill above the cave, rock exposures are common, although the red soil, often up to 0.5 m thick, covers most of the hill surface over the carbonates (Krklec et al., 2016).

Inside Eagle Cave, temperature and relative humidity are measured continuously (Domínguez-Villar et al., 2013). Both temperature and relative humidity have a limited natural seasonality, whereas these parameters exhibit even less variability as a result of the impact of visitors to the cave (Domínguez-Villar et al., 2010). During the period 2009-2013 the average cave temperature was 15.6 ±0.1 ºC (uncertainty accounts for 1 standard deviation of daily data). Reliable relative humidity data has been acquired from 2011 onwards after installing a preheated probe (Vaisala HMP155), providing a relative humidity of 99.2 ± 0.1 %. Water samples were collected in Eagle Cave at 11 drip sites and 3 natural pools (See Table 1 in the supplementary material). In addition, water samples were also collected from one location isolated from any drip where water was left to equilibrate with cave atmosphere moisture. The selection of drip sites considered a wide variety of drip rates and under the studied drip sites there are different types of speleothems, from small candle-like speleothems to flowstones.

3.- Methodology

3.1. Cave water sampling, drip rate monitoring and stable isotope analyses

Cave water samples were collected during 5 years from 2008 until 2013 at uneven intervals, ranging from less than 1 month to 4 months. Drip waters were collected in 30 ml HDPE bottles left under the drips with small plastic funnels to ensure that all drops were collected (Fig. 1C). Depending on the drip rate, certain drip sites permitted collecting samples within some minutes or hours, otherwise bottles were left under the drips until a subsequent visit to the cave 1 to 3 weeks later. For this reason, two visits to the cave were required during every sampling campaign. Even when discharge rates allowed collecting samples within a day, often a bottle was left under those drips until the subsequent visit within each sampling campaign to test any potential bias caused by the sampling protocol. Pool water was collected with syringes. Water collected in the HDPE bottles or with syringes was transferred to 2 ml glass vials and capped with lids having septa. Whenever possible, vials were filled with water to the top taking special caution that no airspace was left under the lid. Collected samples were stored under dark and cold conditions in a fridge (i.e., around 4 ºC) until their analysis. One of the studied pools had relatively constant water level, whereas in other two it varied. One of the pools with variable water level drains completely during part of the year. At least one drip or water flow is assumed to have provided water to the pools. The drainage of the pools is by overflow and/or by seepage, and no evaporation is expected because of the high relative humidity in the cave. Water collected from a cave pool was left to equilibrate with the cave atmosphere moisture in a site with no drips. Several 30 ml bottles were used to contain that water, and more than 6 months were left before the first water aliquot was collected for its analysis. Since the cave atmosphere is saturated with water and air currents are so slow that they were not appreciable during cave visits, these samples are expected to follow the average isotope composition of the cave drips (Domínguez-Villar et al., 2018). Small aliquots (i.e., 2 ml) of the equilibrated water were collected for analysis during sampling campaigns.

Drip rate was measured at seven of the studied sites using Stalagmate drip counters (Collister and Mattey, 2008). Not all drip sites were suitable to use drip counters (i.e., short distance to stalactite). In other cases, when several sites were located very close to each other and show similar discharge, only one of the sites was equipped to optimize resources. In drip sites without continuous monitoring, qualitative data on discharge patterns was obtained based on field observations, including the amount of water collected in every visit to the cave (Fig. 1D; Table 1 in supplementary material). Water stable isotope analyses (δ^2H and $\delta^{18}O$) were conducted at the University of Birmingham using a Isoprime continuous-flow isotope ratio mass spectrometer. The water δ^2H analyses were undertaken using the pyrolysis method over chromium in a Eurovector elemental analyzer at 950 °C, while the $\delta^{18}O$ analyses were undertaken using an equilibration technique in a Isoprime Multiflow. Raw analytical values were corrected for instrumental drift and calibrated using both, internal laboratory standards UOB08 (δ^2H=-40.40; $\delta^{18}O$=-6.56), UOB09 (δ^2H=-157.60; $\delta^{18}O$=-20.87) and UOB10 (δ^2H=-2.82; $\delta^{18}O$=-1.77) that have been calibrated to IAEA standards SLAP, V-SMOW and GISP.

All results are expressed using the δ-notation relative to the Vienna Standard Mean Ocean Water (V-SMOW). The analytical uncertainty (internal precision) was typically <1.5‰ for δ^2H and <0.1 ‰ for $\delta^{18}O$ analyses. Whereas arithmetic isotope averages provide the same weight to each isotope value in a series, weighted isotope averages balance each isotope value by the amount of water contributed to the total amount of water in the averaged series. Thus, weighted averages are calculated during mixing processes in this paper to keep the mass balance of isotope compositions.

3.2. Design of ISODRIP model

We developed a new lumped model (e.g., Fairchild et al., 2006) that considers an atmosphere layer, a soil layer and a vadose zone layer. A sketch of the model is provided in figure 2. The model has a monthly resolution and required data are the monthly time series of amount of precipitation, potential evapotranspiration and $\delta^{18}O$ composition of precipitation, together with a series of soil and karst parameters, as well as the initial values of water amount and its isotope composition in the different reservoirs considered in the system (see Table 2 in the supplementary material). Although one of the time series required is the potential evapotranspiration, the model calculates actual evapotranspiration to have a realistic approach to soil water balance and the magnitude and timing of large recharge events. All units of amount of water (volume) are reported in mm to facilitate the comparison with precipitation, where the unit mm refers to mm/m^2 and that is equivalent to liters. The model is designed for the flow of water under low environmental temperatures, since no water-rock isotope exchanges are considered. So, the model might not be adequate to characterize the karst hydrology under hydrothermal conditions.

Most of the precipitation infiltrates into the soil but a fraction of it is allowed to enter as direct recharge to the epikarst (Fig. 2). Two components of direct recharge are enabled, one that represents a constant proportion of precipitation (R_{d1}) to simulate bedrock exposure at the surface, whereas the second component is a variable proportion depending on the moisture conditions of the soil (R_{d2}) to simulate recharge through cracks or other discontinuities in the soil. The total recharge that enters the vadose zone layer (R_T) flows through the karst drainage system that may include interconnected conduits, fissures, cracks, joints and pores. We have designed a vadose zone drainage system with four different modules that account for different scenarios where particular flow regimes dominate the seepage. Module A is characterized by diffuse flow under normal environmental pressure conditions. Module B represents a diffuse flow drainage that is subject to temporary overpressure conditions. This module simulates drip sites with large variations in discharge rate but a well-mixed isotope signal. Overpressure conditions occur when air in the diffuse flow network does not escape through the vadose zone and soil during soil recharge events, increasing its atmospheric pressure that eventually impacts the drip rate. Module C simulates a drip site that overflows from a storage within the vadose zone that receives water from diffuse and preferential flow networks. The secondary output of this module (drip C_2) is included only to keep the mass balance. The discharge of drip C is continuous due to the diffuse flow component. Thus, although this site never stops dripping, it has large variations in drip rate. Module D simulates the underflow drainage of a storage within the vadose zone that receives water from diffuse and preferential flow networks. The secondary output of this module (drip D_2) is only included to keep the mass balance. This module is allowed to exhaust the storage and provides a discontinuous record. The calculations made in module A are of key importance to other modules, since all of them include at some point a diffuse component in their flow. In module A, not all recharge water enters the diffuse flow network. There is a threshold in the amount of water that can enter this network in every time step as a result of its slow flow rate. Any recharge water that surpasses such threshold is deviated to different modules as overflow water and enters the vadose zone in preferential flow networks such as conduits or open fissures. When the recharge does not overpass the maximum diffuse flow network threshold, most of the recharge enters the vadose zone as diffuse flow, although a fraction of the recharge also enters conduits and open fissures. A detailed description of the model and its mathematical expressions are provided in the supplementary material.

The simulated isotope composition of different drips depends greatly on the parameters selected to run the model. The initial selection of parameters requires the input of estimated values by the operator, unless other sources of information are available (e.g., some parameters such as field capacity or percentage of rock exposure can be measured). Obtaining the final selection of parameters involves a series of trial runs to find the best fit between simulations and observations. During an initial evaluation of the selected parameters, the amount of water in the different reservoirs of the model must reproduce the cave hydrology observations (e.g., drips have continuous or discontinuous flow). A proper evaluation of the hydrological balances of the flow networks or storages considers not only the seasonality but also the inter-annual variability. The next criteria to select the model parameters is the amplitude of isotope variability of the drip waters. To complete the trial runs, the absolute value of drip water isotope composition and its long-term variability are adjusted to select the final model parameters. Since many parameters have a limited range of variability capable to reproduce observations (e.g., to keep a steady state of inter-annual amount of water in the system), simulations are substantially constrained by observations, reducing the impact of the selected parameters by the operator.

4. Results

4.1. Eagle Cave water isotope record

The stable isotope composition ($\delta^{18}O$ and $\delta^{2}H$) of 300 cave water samples was analyzed for this study. Samples were collected during 26 sampling campaigns each of them consisting of two visits to the cave. The high relative humidity measured in the cave (i.e., >98%) is consistent with negligible evaporation processes within the cave, which is supported by the lack of enrichment in oxygen-18 of samples exposed to cave atmosphere during sampling campaigns (Fig. 3A). Most cave waters have a constrained range of isotope values and $\delta^{18}O$-$\delta^{2}H$ relationship. However, we identified a limited number of cave water samples (N=13) that provided anomalous results when compared to the rest of the record within each sampling sites (see text section 1.2 in the supplementary material). Those anomalous samples were not removed from the database or the graphs but were not used in calculations. We compare the isotope composition of cave waters to the local meteoric water line (Fig. 3A). The isotope variability along the local meteoric water line is used to split the cave water sites in two groups: sites with well-mixed waters and sites with partially-mixed waters. The partially-mixed cave waters nicely follow the local meteoric water line, whereas the well-mixed cave waters have a limited variability, although all samples sit on top of the local meteoric water line. So, the isotope signature of the collected cave waters does not record any measurable sign of evaporation in the cave, the vadose zone or the soil.

The $\delta^{18}O$ records show that most cave waters of all sites have an isotope composition that falls within the range of variability of the annually weighted average $\delta^{18}O$ values of precipitation, that during the studied period was 1.83‰ (Fig. 3B). No seasonal $\delta^{18}O$ variability is observed in the partially-mixed or the well-mixed cave waters despite the obvious seasonality in the precipitation $\delta^{18}O$ record (Fig. 3C). The monthly $\delta^{18}O$ variability of precipitation is ~10‰, whereas the partially-mixed cave waters show a variability of ~3‰ and the well-mixed waters have a variability ~1‰. Most of the variability recorded in the well-mixed cave waters corresponds to long-term isotope changes. The long-term trend of the $\delta^{18}O$ record of well-mixed cave waters does not follow a simple smooth and/or delayed signal of the precipitation $\delta^{18}O$ record. However, the good fit of the cave waters isotope signature to the local meteoric water line and its annually weighted isotope composition of precipitation supports the view that water originates from precipitation. Nevertheless, the $\delta^{18}O$ variability of cave waters depends on complex admixtures of precipitation within the karst system that transform the original signal.

4.2. Simulation of the soil water and recharge

Actual evapotranspiration was calculated considering the amount of water available in the soil and the potential evapotranspiration. The results of the calculated actual evapotranspiration show that the hydrological deficit is restricted to four months per year (i.e., May to August), and that ~40% of precipitation is either stored in the soil or enters the vadose zone as recharge, whereas ~60 % of the precipitation is returned to the atmosphere as actual evapotranspiration (Fig. 4A). Because of the direct recharge components, the vadose zone receives recharge every month in which there is precipitation. During the 2009-2013 period, the direct recharge accounted for ~32% of recharge into the vadose zone (Fig. 4B). Thus, most of the recharge occurs when accumulated water in the soil exceeds the field capacity, a component of recharge that in the model is labeled as R_S. The contribution of the R_S component to the total recharge is discontinuous, with only 30% of the months during the studied period having R_S recharge. A clear R_S seasonal pattern is observed during years with abundant precipitation recorded during the rainy season, although during dry years the contribution of R_S is limited and lacks a clear seasonality. Water infiltrated in the soil is accumulated in this reservoir until it is removed by evapotranspiration or is flushed to the vadose zone as recharge. Thus, precipitation that is infiltrated every month in the soil mixes with the water that was already accumulated in that reservoir. The mixing of water in the soil reduces the amplitude of precipitation $\delta^{18}O$ values (i.e., ~10‰) and provides a series of modelled monthly soil water with $\delta^{18}O$ values that varied ~3‰ (Fig. 4C).

During periods when there is Rs, the total recharge can be up to one order of magnitude larger than during periods when all recharge originates from direct recharge components. Most of the water that enters the aquifer when R_S is the prevailing source of recharge goes to preferential flows. Therefore, during large recharge events, only a limited percentage enters the diffuse flow network and contributes to the isotope composition of well-mixed drip waters.

4.3. Simulation of well-mixed cave waters

ISODRIP model considers four different modules within the vadose zone layer. The modules A and B capture the signal of well-mixed cave waters, being A the general case, and B a specific situation that could affect certain drips. Results of the module A show that the amount of water stored in the diffuse flow network of the aquifer above the simulated drip site (A_{DfA}) has a stable long-term signal and a limited intra-annual variability regarding seasonal or inter-annual amount of recharge (Fig. 5A). The discharge of water in the simulated drip site of module A (Q_A) is small and has limited variability, nicely simulating the characteristics of slow and continuous drip sites (Fig. 5B). During recharge events, only a limited amount of water enters the diffusional flow network of Module A (R_{TDf}), whereas any volume of water above the selected threshold is diverted to preferential flows (R_{TPf}). The simulation suggests that the contribution of total recharge to the diffuse flow network (R_{TDf}) is <25% (Fig. 5B), whereas the rest of the recharge is diverted by preferential flows (R_{TPf}). In the diffuse flow network, direct recharge contributions are more frequent than recharge events from soil water, but the latter reach the maximum capacity of recharge that this network can assimilate in every event. Thus, the contribution to total recharge that enters the diffuse flow drainage network is equally distributed (~50%) between direct recharge (R_d) and soil water recharge (R_S). These results support that the direct recharge has a major role in controlling the hydrology of the diffuse flow system and cannot be ignored.

The module A of ISODRIP simulates the isotope composition of water at the top of the diffuse flow network in the vadose zone (δ_{DfA}) that accounts for the mixing of recharge and underground water. The residence time [transit time] of water in [through] the diffuse flow network is given by the ratio between the accumulated water in the network and the discharge. According to ISODRIP, the residence time of water in the diffuse flow network of Eagle Cave is on average 15 months. Once this parameter is known the isotope composition of the network at the top of the aquifer is mixed and transferred to the simulated drip site. Thus, the $\delta^{18}O$ composition of the simulated drip in module A (δ_A) is a smoothed and delayed signal of the water at the top of the diffuse flow network in the vadose zone (δ_{DfA}). In Eagle Cave, the simulated drip water isotope composition lacks any seasonality, as expected from the estimated residence time, although the larger changes in $\delta^{18}O$ still can occur within less than a year.

Some of the monitored drip sites have well-mixed waters according to their isotope signature, although they also have highly variable drip rates. The well-mixed isotope composition of the drip waters supports that the source of water is from the diffuse flow network. However, the fast discharge rates recorded in some sites would exhaust the limited capacity of the water network in module A. However, for these cases we have developed the particular case of module B, that allows lateral flow within the diffuse flow network. In this module, enhanced drip rates are not the results of preferential flow, but overpressure conditions in the diffuse flow network during recharge events that prevents the flow of air in the network to be equilibrated with atmospheric pressure at the surface. The simulation supports changes of drip rate larger than one order of magnitude without exhausting the water in the diffuse flow network (Fig. 5C). However, since this drainage module allows lateral flow and creates temporal hydrological depression cones, it is obvious that this module cannot be a dominant drip site system without affecting the general pattern of surrounding drip sites. In Eagle Cave, the module B drainage system was only assigned to three drips clustered in a small chamber, whereas all other drips associated to diffusional flow were characterized by the module A drainage system.

The faster discharge rate enables more water to enter the diffuse network during large recharge events. Since such recharge events often have more negative $\delta^{18}O$ values, the isotope composition of the water at the top of the diffuse flow network in the vadose zone (δ_{DfB}) and the isotope composition of the drip water (δ_B) have a slight bias towards more negative $\delta^{18}O$ values (Fig. 5D). The maximum $\delta^{18}O$ differences between the simulated drip A and drip B (~0.3‰) occurred after 2010, a year that was unusually wet and had more negative $\delta^{18}O$ values of precipitation. Aside from slight biases in the $\delta^{18}O$ signal, both modules follow a similar structure during the modelled period.

4.4. Simulation of partially-mixed cave waters

To simulate the $\delta^{18}O$ signal of partially-mixed cave water, ISODRIP incorporates two modules (C and D) that represent preferential flow drainages that pass through different storages were preferential and diffuse water drainages interact. Module C represents the overflow of a storage that results in a drip with continuous flow. Module D represents the underflow of a storage that results in a drip with discontinuous flow. The designed hydrological network has secondary outflow routes in each module (drip C2 and drip D2). These outflow drainages are essential to enable hydrological stability to the main module drips replicating the observed dynamics in Eagle Cave, although they are not the focus of the simulation in the module.

The discharge of the main drip of module C captures the overflow drainage of a storage (SC) that accumulates water from preferential and diffusional flows. Discharge of this drip (Q_C) has a high flow rate when preferential water overflows the storage, while records a limited drip rate otherwise. The transition between flow rates is sharp (Fig 6A). However, the amount of water in the storage (A_{SC}) is relatively stable, with sharp increases when preferential flow operates and gradual decreases otherwise due to the diffuse outflow drainage. The $\delta^{18}O$ composition of the storage (δ_{SC}) and the drip (δ_C) have a range of 2.5‰ with more negative values when preferential flows trigger higher drip rates, and $\delta^{18}O$ values more similar to those in the module A when diffuse flow drainage dominate the discharge (Fig. 6B). The model captures nicely the magnitude of the isotopic anomalies and the timing of some of them, but fails to predict every single isotope negative anomaly. This hydrological design does not simulate isotope anomalies less negative than those simulated by modules A and B, and consequently does not reproduce the full set of partially-mixed $\delta^{18}O$ values recorded.

The discharge of the main drip of module D (Q_D) captures the drainage of a storage (S_D) that accumulates water from preferential and diffusional flow drainages. In this case, S_D has an underflow that enables the complete drain out of the storage sometime after the preferential flow drainage ceased. In this module, the discharge of the main drip of the module (Q_D) provides more gradual transitions after the flow through preferential drainages ceases and the drip stops once the storage drains out completely. The simulated discharge reproduces the discontinuous drip pattern observed in several drips in Eagle Cave (Fig. 6C). The $\delta^{18}O$ composition of the storage (δ_{SD}) and the drip (δ_D) have a range of 3‰ (Fig. 6D). The simulation is a discontinuous time series that sometimes shares variability with the well-mixed cave water $\delta^{18}O$ signal but also has important anomalies around it. Most of the anomalies provide more negative $\delta^{18}O$ excursions, although this module also simulates less negative $\delta^{18}O$ anomalies in relation to well-mixed cave water $\delta^{18}O$ signal. Although δ_D covers most of the range of isotope variability recorded in Eagle Cave, the timing of events is difficult to replicate accurately.

4.5. Comparison of observed and simulated cave water $\delta^{18}O$ records

Sampling sites were characterized according to their hydrological and isotope variability to different modules of ISODRIP (see Table 1 in supplementary material). The simulated $\delta^{18}O$ signals of drips A, B, C and D were compared with the observed $\delta^{18}O$ data of those sites represented within each module. Simulations of drip sites C and D were compared with measured waters from all sites that had partially-mixed $\delta^{18}O$ records, regardless if they were characterized as overflow or underflow drainages. The module A, that simulates a drip characterized by a diffuse flow drainage, is represented in the cave by seven of the monitored sites. The simulated $\delta^{18}O$ signal of drip A has the highest correlation when compared to the $\delta^{18}O$ observations ($r = 0.82$; p-value <0.005) and explains 68% of the variance of the $\delta^{18}O$ observations (Fig. 7). The range between the confidence intervals of the regression overlaps with the uncertainty of observations in all samples except one, although in this case, only two sites were available to characterize the variability of all cave waters during that month. However, this regression has discarded three months ($N=25$) that were clear outliers. A justification for the removal of these outliers is provided in the supplementary material. Module B also characterizes diffusional flow drainages, although in this case, overpressure conditions during recharge events enable highly variable drip rates. Three of the monitored drip sites, all of them located in the cave within one square meter, were characterized under this drainage regime (Fig. 1C). The correlation coefficient between the simulated drip B $\delta^{18}O$ signal and the observed $\delta^{18}O$ record is also high ($r = 0.76$, p-value <0.005) and explains 58% of the variance of observed data (Fig. 7). All observations considering their uncertainties overlap with the range between the confidence intervals of the regression, although from 17 observations two were clear outliers and were removed from the analysis.

Module C, that represents an overflow storage drainage, has the lowest correlation between simulated and observed $\delta^{18}O$ data ($r = 0.56$, p-value <0.005) and explains 31% of the variance of $\delta^{18}O$ observations (N=26) (Fig. 7). All sites with partially-mixed $\delta^{18}O$ signal were used for the comparison (5 sites; see Table 2 in the supplementary material). However, it is not clear that any of the studied drip sites will be dominated by this kind of flow regime. No data were removed from the dataset despite an outlier is recorded, since no clear justification was found to discard the values of that month. Module D, that represents an underflow storage drainage, has an unexpectedly high correlation coefficient between simulated and observed $\delta^{18}O$ data ($r = 0.73$, p-value <0.005) and explains 54% of the variance of the observations (Fig. 7). However, it has to be kept in mind that the simulation considers a discontinuous record and that the period of flow of different observed sites not always coincides with the simulated drip site, limiting the number of observations (N=15). Although the simulated and observed $\delta^{18}O$ values do not record outliers, when considering the uncertainties of observations two data points do not fit within the range between the confidence intervals of the regression.

5. Discussion

5.1. Implementation of ISODRIP model to Eagle Cave

The hydrological results of ISODRIP model capture the structure of the main drips monitored in Eagle Cave as well as reproduce the mean value and variability of the $\delta^{18}O$ record. The simulation suggests that the mean residence time of the diffuse flow in the main chamber of the cave is on average 15 months and captures very well the inter-annual $\delta^{18}O$ variability, including the exceptionally more negative $\delta^{18}O$ values of precipitation during the year 2010. However, the simulated $\delta^{18}O$ signal provides a slightly smoother signal than the observations. The simulations of modules A and B assume a pure diffusional flow, whereas the real hydrology of the system is likely to be more complex. Thus, although many of the studied sites are dominated by diffuse flow drainages, this does not prevent the existence of secondary sources from preferential flows that could interact at any point during the transit time with the diffuse flow network, increasing its $\delta^{18}O$ variability.

Models with preferential flow drainage are more complex to evaluate. Five sites recorded cave water with partially-mixed $\delta^{18}O$ values suggesting that those sites were dominated by preferential flow regimes. We designed module C to provide a continuous flow and module D to produce a discontinuous flow. The monitoring of three drips showed that after each wet season, when all the sites suddenly increase their discharge, they progressively decrease their drip rate until eventually dry out. This gradual decrease of discharge suggests an underflow drainage (module D). However, since there is no evaporation in the cave, hydrologically there is no clear way to determine if the pool water is sourced predominantly from overflow (module C) or underflow drips (module D). The simulations of preferential flows show that values less negative than the $\delta^{18}O$ signal simulated with modules A and B are only possible when implementing the module D (not the module C). Since all monitored sites that record partially-mixed waters have in their time series $\delta^{18}O$ values less negative than the simulations of modules A and B, the model supports that all studied sites having significant preferential flows are better characterized by module D: an underflow drainage regime (Fig. 8). Since the cave has thousands of drip sites, is likely that many of them would be dominated by overflow drainage regimes, but none of the 15 sites that we selected for this study provided signals compatible with that regime. The correlation of the observed $\delta^{18}O$ record of sites with partially-mixed waters and the simulated $\delta^{18}O$ signals of the modelled drip site D is relatively high. However, since the simulated drip D provides a discontinuous record that not always coincides with the periods of discharge in the different monitored sites, the overall time series (Fig. 6D) suggests that the good fit of the simulation and observations might be overestimated.

The calculated actual evapotranspiration suggests that during the studied period ~60% of the precipitation returned to the atmosphere by evaporation or transpiration. This distinction is important, because evaporation is a process that results in kinetic fractionation whereas transpiration does not (Gat, 2010). Therefore, although we do not record evaporation in the cave, it is obvious that a significant fraction of water was evaporated while stored in the soil, before recharge events flushed it into the epikarst to participate into every drip water in the cave. However, the isotope signature of water collected in Eagle Cave does not record any sign of significant evaporation in relation to the local meteoric water line. The lack of evaporative signature in the isotope signal is common to cave waters from regions with very different climates. To reproduce realistic cave water $\delta^{18}O$ signals, models often use unrealistically low fractionation factors (Wackerbarth et al., 2010; Treble et al., 2013), whereas other simply ignore the evaporation processes in the soil (Partin et al., 2012; Moerman et al., 2014; Domínguez-Villar et al., 2018; Jean-Baptiste et al., 2019). ISODRIP model follows the latter approach regarding isotope fractionation in the soil. Although the remaining soil water fraction would have higher $\delta^{18}O$ values, major precipitation events responsible for triggering recharge have often relatively low $\delta^{18}O$ values, minimizing the impact of evaporation in soil water (Dansgaard, 1964; Gat, 1996; Lachniet et al., 2009). In addition, dew produced from condensation of atmospheric moisture (Aravena et al., 1989) or even dew originated from soil water moisture (Kaseke et al., 2017) likely counteract part of the evaporative $\delta^{18}O$ biases. Therefore, it is not unusual that shallow underground water would be used as a good approximation to the long-term weighted isotope composition of precipitation, as is the case in Spain (Plata, 1994).

Water left to equilibrate with the moisture of the cave atmosphere has a $\delta^{18}O$ signal that follows the well-mixed cave waters. Since drainage through the diffuse flow network better reproduces the isotope observations, the recorded $\delta^{18}O$ variability in equilibrated water samples suggests that diffuse flow networks provide most of the moisture to the cave atmosphere. However, the reality is slightly more complex. The implementation of ISODRIP in Eagle Cave supports that >75% of recharge flows through the preferential flow network characterized by having partially-mixed $\delta^{18}O$ signals. However, not even during large events of recharge the $\delta^{18}O$ signal of the cave atmosphere is significantly affected, as recorded by the water samples equilibrated with the atmosphere. The site where equilibrated samples were collected is far from major preferential flow drainages (e.g., major flowstones), although the advection in the main hall tends to homogenize the atmosphere (Domínguez-Villar et al., 2013) limiting any local impact. The $\delta^{18}O$ values of cave waters that deviate from the well-mixed isotope signature are short-lived and the timing of enhanced discharge that goes along with such deviations differs greatly depending on flow routes. Therefore, waters with partially-mixed $\delta^{18}O$ signals smooth their anomalies into the dominant $\delta^{18}O$ signal (i.e., well-mixed cave waters). In Eagle Cave, the water equilibrated with the cave atmosphere is impacted by both, diffuse and preferential flow drainages, although individual drip anomalies are smoothed resulting in a well-mixed $\delta^{18}O$ signal comparable to the one recorded by drainages of the diffuse flow network (Fig. 3C). Similar observations were reported in a different cave where evaporation in the studied chamber is also negligible (Domínguez-Villar et al., 2018).

5.2. Implications of ISODRIP model to paleoclimate research

During the last decade, drip water isotope modelling has shown that in caves without evaporation recorded in the cave water $\delta^{18}O$ signal, different drips can result in very different signals despite having the same input parameters (e.g., Baker et al., 2012). For this reason, replication of speleothems is essential to evaluate which speleothem $\delta^{18}O$ anomalies can be attributed to changes in the climate/environment and which $\delta^{18}O$ anomalies fall in the natural range of $\delta^{18}O$ variability within a cave caused from different flow routes in the vadose zone (e.g., Jex et al., 2013; Hercman et al., 2020). Speleothem paleoclimate researchers often assume that outside the tropics, the speleothem $\delta^{18}O$ records, as well as the vadose zone water, have $\delta^{18}O$ compositions biased towards winter (e.g., Pape et al., 2010; Moreno et al., 2014), because of the limited recharge during summer months due to enhanced evapotranspiration and in some cases also the limited precipitation. This could justify a theoretical correlation between speleothems and winter climate indexes (Baldini et al., 2008; Deininger et al., 2016), although speleothem records from Europe do not support the assumption of a strong recharge bias towards winter (Mischel et al., 2015). On the other hand, in tropical regions, drip water $\delta^{18}O$ signal of some caves has been suggested to be biased towards the summer monsoon season, because this is when most of the recharge takes place (Partin et al., 2012; Breitenbach, 2015). However, drip water often records mean drip $\delta^{18}O$ values very close to the weighted isotope composition of the precipitation (Moerman et al., 2014; Duan et al., 2016). Therefore, observations do not support a systematic bias of drip water $\delta^{18}O$ signal, in comparison with the mean weighted isotope composition of precipitation, towards the season with larger recharge.

Some cave water $\delta^{18}O$ models assume direct flow of precipitation into the aquifer (Partin et al., 2012; Genty et al., 2014; Moerman et al., 2014; Mischel et al., 2015; Jean-Baptiste et al., 2019). However, soil is an efficient filter that controls recharge and greatly impacts the recharge $\delta^{18}O$ composition (Comas-Bru et al., 2015). So, more sophisticated $\delta^{18}O$ hydrological models include a soil layer (e.g., Wackerbarth et al., 2010; Treble et al., 2013; Domínguez-Villar et al., 2018). ISODRIP is the first cave water $\delta^{18}O$ model to account for direct recharge components as well as having a soil layer. This innovation enables every single month with precipitation to account for the cave water $\delta^{18}O$ composition regardless of the existence of seasonality in the major recharge events. Including a direct recharge component is a more realistic approach for many karst aquifers, since rock exposures are common in karst landscapes. This feature of the model is particularly important when applied to Mediterranean and semiarid/arid environments. Under these climates, soil cover is often discontinuous and rock exposures represent large percentages of land surface, allowing a fraction of precipitation to enter the vadose zone without passing through the soil filter. So, for sites where direct recharge takes place, all significant precipitation events affect the cave water $\delta^{18}O$ composition independently of the month in which they occur.

There is another hydrological phenomenon that limits the impact of large seasonal recharge events biasing the average drip $\delta^{18}O$ signals in relation to the mean weighted

$\delta^{18}O$ composition of precipitation. Soil recharge events often involve larger volume of water that cannot be assimilated at once by the diffuse flow drainage network. So, during large recharge events, most of the recharge is transferred underground by preferential flow networks (i.e., conduits and fissures). So, only drips dominated by preferential flow drainages will record certain $\delta^{18}O$ bias towards periods of recharge, whereas those drips dominated by diffuse flow would have a minimal impact. A maximum threshold for the amount of recharge entering the diffuse flow network was already implemented in previous cave water $\delta^{18}O$ models (e.g., Jean-Baptiste et al., 2019) and this feature is also included in ISODRIP. Thus, the impact of direct recharge and the maximum threshold of the aquifer to assimilate recharge water, explain the good fit of many cave water $\delta^{18}O$ values with the annually weighted average $\delta^{18}O$ values of precipitation in caves from different climates (Goede et al., 1982; Yonge et al., 1985; Caballero et al., 1996; Fleitmann et al, 2004; Lambert and Aharon, 2010). Considering the processes described above, we do not support the idea that climate over the cave controls a systematic bias of drip water $\delta^{18}O$ values in relation to mean weighted $\delta^{18}O$ values of precipitation (Baker et al., 2019). Instead, drip sites dominated by preferential flow routes as well as drip sites with evaporative processes within the vadose zone are likely to be behind most divergences.

Cave water studies have demonstrated that understanding the role of evaporation in cave waters is critical to properly interpret the variability of speleothem $\delta^{18}O$ records (Cuthbert et al., 2014; Feng et al., 2014). In addition, cave water $\delta^{18}O$ models have demonstrated that for the same cave, multiple drip $\delta^{18}O$ signals with a wide compositional range can be the result of different flow routes (Fig. 8). The $\delta^{18}O$ variability related to different flow routes may be larger than the amplitude expected for large climate anomalies such as Younger Dryas (Baker et al., 2013). Thus, instead of doing general assumptions, to properly understand a speleothem $\delta^{18}O$ record, it is critical to characterize the hydrology of the drip site that formed the studied speleothem, as well as its relationship with the mean weighted $\delta^{18}O$ signal of precipitation. Nevertheless, particular drips might have non-stationary dynamics (Moerman et al., 2014), and not in all cases the monitoring results could be extrapolated to the past. Sometimes there is no certainty in linking speleothems and specific drip sites or is obvious that the drip dynamics have changed through time (e.g., changes in flow route due to micro-collapses within the vadose zone or filling of fissures/porosity by detrital/chemical deposits). In these cases, replication of various speleothem records covering the same time period is recommended to evaluate the variability of $\delta^{18}O$ in the cave/chamber (e.g., Domínguez-Villar et al., 2017; Hercman et al., 2020). The replication of multiple speleothem records is time and resource consuming, but provides a reliable signal and narrows down the impact of hydrology in the composite $\delta^{18}O$ record variability. Replication studies are important independently of the goal of the speleothem research being on meteorological events such as hurricanes or cyclones (e.g., Partin et al., 2012) or on long-term climate changes. Most replication test are typically designed to constrain the impact of kinetic fractionation (Dorale and Liu, 2009) and frequently only two speleothems are compared (e.g., Wang et al., 2001). However, to characterize the variability of paleo drip water $\delta^{18}O$ signature in a cave/chamber based on speleothem $\delta^{18}O$ records, replications based on more than two speleothems are desirable. In any case, $\delta^{18}O$ models of drip waters suggest that to prevent misinterpreting anomalies in speleothem $\delta^{18}O$ records, replication should become a common practice in paleoclimate studies not just to evaluate kinetic effects, but also to understand the internal variability introduced in the signal by the karst hydrology.

6. Conclusions

We have developed a new cave water isotope hydrological model (ISODRIP) that captures not only the mean $\delta^{18}O$ composition of observed drip water and its variability, but also reproduces nicely the inter-annual variability of the signal. ISODRIP considers four different flow scenarios to capture diffuse and preferential flow drainages in the system. Module A characterizes drips with diffuse flow under atmospheric pressure conditions. Drips with limited drip rate variability and a well-mixed drip water $\delta^{18}O$ signals should be simulated with this module. Module B characterizes drips with diffuse flow under temporal overpressure conditions. Drip sites with large drip rate variations and well-mixed drip water $\delta^{18}O$ signals should be simulated with this module. Module C represents drips with diffusional and preferential flows passing through an overflow storage. Drip sites with a continuous and very variable discharge that record partially-mixed $\delta^{18}O$ signals should be simulated with this module. Finally, module D represents drips where diffuse and preferential flows circulate through a underflow storage. Drip sites with a discontinuous record and partially-mixed $\delta^{18}O$ signals should be simulated with this module. Each module can be adjusted to reproduce as many virtual drip sites as desired. The simulations include a direct recharge component in the soil layer that enables precipitation from any significant event to contribute to the cave water oxygen isotope composition. Therefore, we provide evidence to support that recharge is unlikely to be limited to certain periods of the year (e.g., winter), including in Mediterranean, semiarid or even arid climates unless in specific drip sites dominated by preferential flows. The best fit of our simulated and observed $\delta^{18}O$ signals is for diffuse flow drainages. In these cases, the simulations suggest that in Eagle Cave the average residence time of water in the vadose zone above the cave is 15 months. The relative humidity in Eagle Cave is always nearly 100% and consequently no evaporation is recorded in the cave water $\delta^{18}O$ record in relationship to the local meteoric water line. Water exposed to the moisture of the cave atmosphere records a well-mixed $\delta^{18}O$ signal similar to water from diffuse flow drainages, since the anomalies introduced by the preferential flow drainages are not synchronous and are progressively smoothed.

We described the conditions for diffuse flow drainages to be capable to provide well-mixed $\delta^{18}O$ signals even when discharge rates increase exponentially as a response to recharge events. The module that simulates such conditions enables a temporary lateral water flow component for particular drip sites where pressure builds up in the drainage network during recharge events. Simulation of preferential flow drainages is more complex to reproduce, although the magnitude of $\delta^{18}O$ events was properly captured. The monthly timescale of the model is likely insufficient to simulate accurately the flow through preferential conduits and its interaction with different storage components, although provides a good approximation to the average $\delta^{18}O$ composition of cave waters and its variability.

Acknowledgements

The research leading to these results has received funding from the European Community under a Marie Curie Intra-European Fellowship of the Seventh Framework Programme FP7/2007-2013 (grant agreement nº 219891; PROCAVET project). This research received funds from the project “Inter-comparison of karst denudation measurement methods” (KADEME) (IP-2018-01-7080) financed by Croatian Science Foundation. We

thank the suggestion of four anonymous reviewers that improved the original version of this manuscript.

REFERENCES

Aravena, R., Suzuki, O., Pollastri, A., 1989. Coastal fog and its relation to groundwater in the IV region of northern Chile. Chemical Geology 79, 83-91.

Arbel, Y., Greenbaum, N., Lange, J., Inbar, M., 2010. Infiltration processes and flow rates in developed karst vadose zone tracers in cave drips. Earth Surface Processes and Landforms 35, 1682-1693.

Ayalon, A., Bar-Matthews, M., Sass, E., 1998. Rainfall-recharge relationships within a karstic terrain in the Eastern Mediterranean semi-arid region, Israel: $\delta^{18}O$ and δD characteristics. Journal of Hydrology 207, 18–31.

Baker, A., Bradley, C., 2010. Modern stalagmite $\delta^{18}O$: instrumental calibration and forward modelling. Global and Planetary Change 71, 201–206.

Baker, A., Bradley, C., Phillips, S.J., 2013. Hydrological modeling of stalagmite $\delta^{18}O$ response to glacial-interglacial transitions. Geophysical Research Letters 40, 3207–3212.

Baker A., Bradley, C., Phillips, S.J., Fischer, M., Fairchild, I.J., Fuller, L., Spötl, C., Azcurra, C., 2012. Millennial-length forward models and pseudoproxies of stalagmite $\delta^{18}O$: an example from NW Scotland. Climate of the Past 8, 1153-1167.

Baker, A., Fairchild, I.J., 2012. Drip water hydrology and speleothems. Nature Education Knowledge 3(10), 16.

Baker, A., Hartmann, A., Duan, W., Hankin, S., Comas-Bru, L., Cuthbert, M.O., Treble, P.C., Banner, J., Genty, D., Baldini, L.M., Bartolomé, M., Moreno, A., Pérez-Mejías, C., Werner, M., 2019. Global analysis reveals climatic controls on the oxygen isotope composition of cave drip water. Nature Communications 10, 2984.

Baldini, L.M., McDermott, F., Foley, A.M., Baldini, J.U.L., 2008. Spatial variability in the European winter precipitation $\delta^{18}O$-NAO relationship: implications for reconstructing NAO-mode climate variability in the Holocene. Geophysical Research Letters 35, L04709.

Bar-Matthews, M., Ayalon, A., Matthews, A., Sass, E., Halicz, L., 1996. Carbon and oxygen isotope study of active water-carbonate system in a karstic Mediterranean cave: implications for paleoclimate research in semiarid regions. Geochimica et Cosmochimica Acta 60, 337-347.

Bradley, C. Baker, A., Jex, C.N., Leng, M.J., 2010. Hydrological uncertainties in the modelling of cave drip-water $\delta^{18}O$ and the implications for stalagmite paleoclimate reconstructions. Quaternary Science Reviews 29, 2201-2214.

Breitenbach, S.F.M, Lechleitner, F.A., Meyer, H., Diengdoh, G., Mattey, D., Marwan, N., 2015. Cave ventilation and rainfall signals in dripwater in a monsoonal setting- a monitoring study from NE India. Chemical Geology 402, 111-124.

Caballero, E., Jiménez de Cisneros, C., Reyes, E. 1996. Applied Geochemistry 11, 583-587.

Carrasco, F., Andreo, B., Liñán, C., Mudry, J., 2006. Contribution of stable isotopes to the understanding of the unsaturated zone of a carbonate aquifer (Nerja Cave, southern Spain). Comptes Rendus Geoscience 338, 1203-1212.

Chapman, J.B., Ingraham, N.L., Hess, J.W., 1992. Isotopic investigation of infiltration and unsaturated zone flow processes at Carlsbad Cavern, New Mexico. Journal of Hydrology 133, 343-363.

Collister, C., Mattey, D., 2008. Controls on water drop volume at speleothem drip sites: An experimental study. Journal of Hydrology 358, 259-267.

Comas-Bru, L., McDermott, F., 2015. Data-model comparison of soil-water $\delta^{18}O$ at a temperate site in N. Spain with implications for interpreting speleothem $\delta 1^{8}O$. Journal of Hydrology 530, 216–224.

Cuthbert, M.O., Rau, G.C., Andersen, M.S., Roshan, H., Rutlidge, H., Marjo, C.E., Markowska, M., Jex, C.N., Graham, P.W., Mariethoz, G., Acworth, R.I., Baker, A., 2014. Evaporative cooling on speleothem drip water. Scientific Reports 4, 5162.

Dansgaard, W., 1964. Stable isotopes in precipitation. Tellus 16, 436–468.

Deininger, M., Werner, M., McDermott, F., 2016. North Atlantic oscillation controls on oxygen and hydrogen isotope gradients in winter precipitation across Europe; implications for paleoclimate research. Climate of the Past 12, 2127-2143.

Domínguez-Villar, D., Fairchild, I.J., Baker, A., Carrasco, R.M., Pedraza, J., 2013. Reconstruction of cave temperature based on surface atmosphere temperature and vegetation changes: implications of speleothem palaeoclimate records. Earth and Planetary Science Letters 369–370, 158–168.

Domínguez-Villar, D., Fairchild, I.J., Carrasco, R.M., Pedraza, J., Baker, A., 2010. The effect of visitors in a touristic cave and the resulting constraints on natural thermal conditions for palaeoclimate studies (Eagle Cave, Central Spain). Acta Carsologica 39, 491-502.

Domínguez-Villar, D., Krklec, K., López-Sáez, J.A., Sierro, F.J., 2020. Thermal impact of Heinrich stadials in cave temperature and speleothem oxygen isotope records. Quaternary Research 1-14, doi:10.1017/qua.2020.99.

Domínguez-Villar, D., Lojen, S., Krklec, K., Baker, A., Fairchild, I.J., 2015. Is global warming affecting cave temperatures? Experimental and model data from a paradigmatic case study. Climate Dynamics 54, 569–581.

Domínguez-Villar, D., Lojen, S., Krklec, K., Kozdon, R., Edwards, R.L., Cheng, H., 2018. Ion microprobe δ^{18}O analyses to calibrate slow growth rate speleothem records with regional δ^{18} records of precipitation. Earth and Planetary Science Letters 482, 367–376.

Domínguez-Villar, D., Wang, X., Krklec, K., Cheng, H., Edwards, R.L., 2017. The control of the tropical North Atlantic on Holocene millennial climate oscillations. Geology 45, 303-306.

Dorale, J.A., Liu, Z., 2009. Limitations of Hendy test criteria in judging the paleoclimatic suitability of speleothems and the need for replication. Journal of Cave and Karst Studies 71, 73-80.

Duan, W., Ruan, J., Luo, W., Li, T., Tian, L., Zeng, G., Zhang, D., Bai, Y., Li, J., Tao, T., Zhang, P., Baler, A., Tan, M., 2016. The transfer of seasonal isotopic variability between precipitation and drip water at eight caves in the monsoon regions of China. Geochimica et Cosmochimica Acta 183, 250-266.

Even, H., Carmi, I., Magaritz, M., Gerson, R., 1986. Timing the transport of water through the upper vadose zone in a karstic system above a cave in Israel. Earth Surface Processes and Landforms 11, 181-191.

Fairchild, I.J., Baker, A., 2012. Speleothem Science: From Process to Past Environments. John Wiley-Blackwell, Oxford.

Fairchild, I.J., Tuckwell, G.W., Baker, A., Tooth, A.F., 2006. Modelling of dripwater hydrology and hydrochemistry in a weakly karstified aquifer (Bath, UK): Implications for climate change studies. Journal of Hydrology 321, 213-231.

Feng, W., Casteel, R.C., Banner, J.L., Heinze-Fry, A., 2014. Oxygen isotope variations in rainfall, drip-water and speleothem calcite from a well-ventilated cave in Texas, USA: Assessing a new speleothem temperature proxy. Geochimica et Cosmochimica Acta 127, 233-250.

Fitts, C.R., 2012. Growndwater Science (2nd edition). Academic Press, Elsevier, Waltham, MA, 696 pp.

Fleitmann, D., Burns, S.J., Neff, U., Mudelsee, M., Mangini, A., Matter, A., 2004. Palaeoclimatic interpretation of high-resolution oxygen isotope profiles derived from annually laminated speleothems from Southern Oman. Quaternary Science Reviews 23, 935-945.

Fuller, L., Baker, A., Fairchild, I.J., Spötl, C., Marca-Bell, A., Dennis, P.F., 2008. Isotope hydrology of dripwaters in a Scottish cave and implications for stalagmite paleoclimate research. Hydrology and Earth System Sciences 12, 1065-1074.

Gat, J.R., 1996. Oxygen and hydrogen isotopes in the hydrological cycle. Annual Review of Earth and Planetary Sciences 24, 225–262.

Gat, J.R., 2010. Isotope Hydrology: A Study of the Water Cycle. Imperial College Press, London.

Gehrels, J.C., Peeters, J.E.M., de Vries, J.J., Dekkers, M., 1998. The mechanism of soil water movements as inferred from 18O stable isotope studies. Hydrological Sciences Journal 43, 579-594.

Genty, D., Labuhn, I., Hoffmann, G., Danis, P.A., Meste, O., Bourges, F., Wainer, K., Massault, M., Van Exter, S., Régnier, E., Orengo, P., Falourd, S., Minster, B., 2014. Rainfall and cave water isotope relationships in two South-France sites. Geochimica et Cosmochimica Acta 131, 323–343.

Goede, A., Green, D.C., Harmon, R.S., 1982. Isotopic composition of precipitation, cave drips and actively forming speleothems at three Tasmanian cave sites. Helictite 20, 17-27.

Hercman, H., Gąsiorowski, M., Pawlak, J., Błaszczyk, M., Gradiński, M., Matoušková, S., Zawidzki, P., Bella, P., 2020. Atmospheric circulation and the differentiation of precipitation sources during the Holocene inferred from five stalagmite records from Demänová Cave System (Central Europe). The Holocene 30, 834-846.

Jean-Baptiste, P., Genty, D., Fourré, E., Régnier, E., 2019. Tritium dating of dripwater from Villars Cave (SW-France). Applied Geochemistry 107, 152-158.

Jex, C.N., Phillips, S.J., Baker, A., Bradley, C., 2013. Reducing uncertainty in the climatic interpretations of speleothem $\delta^{18}O$. Geophysical Research Letters 40, 2259–2264.

Kaseke, K.F., Wang, L., Seely, M.K., 2017. Nonrainfall water origins and formation mechanisms. Science Advances 3, e1603131.

Kaufman, A., Bar-Matthews, M., Ayalon, A., Carmi, I., 2003. The vadose flow above Soreq Cave, Israel: a tritium study of the cave waters. Journal of Hydrology 273, 155-163.

Kluge, T., Riechelmann, D.F.C., Wieser, M., Spötl, C., Sültenfuß, J., Schröder-Ritzrau, A., Niggemann, S., Aeschbach-Hertig, W., 2010. Dating cave drip water by tritium. Journal of Hydrology 394, 396–406.

Krklec, K., Domínguez-Villar, D., 2014. Quantification of the impact of moisture source regions on the oxygen isotope composition of precipitation over Eagle Cave, central Spain. Geochimica et Cosmochimica Acta 134, 39–54.

Krklec, K., Domínguez-Villar, D., Carrasco, R.M., Pedraza, J., 2016. Current denudation rates in dolostone karst from central Spain: Implications for the formation of unroofed caves. Geomorphology 264, 1-11.

Lachniet, M.S., 2009. Climatic and environmental controls on speleothem oxygen-isotope values. Quaternary Science Reviews 28, 412-432.

Lambert, W.J., Aharon, P., 2010. Oxygen and hydrogen isotopes of rainfall and dripwater at DeSoto Caverns (Alabama, USA): Key to understanding past variability of moisture transport from the Gulf of Mexico. Geochimica et Cosmochimica Acta 74, 846-861.

Liñán, C., del Rosal, Y., Carrasco, F., Vadillo, I., Benavente, J., Ojeda, L., 2018. Highlighting the importance of transitional ventillation regimes in the management of Mediterranean show caves (Nerja-Pintada system, southern Spain). Science of the Total Environment 631-632, 1268-1278.

Markowska, M., Baker, A., Andersen, M.S., Jex, C.N., Cuthbert, M.O., Rau, G.C., Graham, P.W., Rutlidge, H., Mariethoz, G., Marjo, C.E., Treble, P.C., Edwards, N., 2016. Semi-arid zone caves: evaporation and hydrological controls on $\delta^{18}O$ drip water composition and implications for speleothem paleoclimate reconstructions. Quaternary Science Reviews 131, 285–301.

Mischel, S.A., Scholz, D., Spötl, C., 2015. $\delta^{18}O$ values of cave drip water: a promising proxy for the reconstruction of the North Atlantic Oscillation? Climate Dynamics 45, 3035.

Moerman, J.W., Cobb, K.M., Partin, J.W., Meckler, A.N., Carolin, S.A., Adkins, J.F., Lejau, S., Malang, J., Clark, B, Tuen, A.A., 2014. Transformation of ENSO-related rainwater to dripwater $\delta^{18}O$ variability by vadose water mixing. Geophysical Research Letters 41, 7907-7915.

Moore, G.W., Sullivan, G.N., 1978. Speleology: the Study of Caves. Zephyrus Press, Teaneck, NJ (USA).

Moreno, A., Sancho, C., Bartolomé, M., Oliva-Urcia, B., Delgado-Huertas, A., Estrela, M.J., Corell, D., López-Moreno, J.I., Cacho, I., 2014. Climate controls on rainfall isotopes and their effects on cave drip water and speleothem growth: the case of Molinos cave (Teruel, NE Spain). Climate Dynamics 43, 221–241.

Pape, J.R., Banner, J.L., Mack, L.E., Musgrove, M., Guilfoyle, A., 2010. Controls on oxygen isotope variability in precipitation and cave drip waters, central Texas, USA. Journal of Hydrology 385, 203-215.

Partin, J.W., Jenson, J.W., Banner, J.L., Quinn, T.M., Taylor, F.W., Sinclair, D., Hardt, B., Lander, M.A., Bell, T., Miklavič, B., Jocson, J.M.U., Taboroši, D., 2012.

Relationship between modern rainfall variability, cave dripwater, and stalagmite geochemistry in Guam, USA. Geochemistry, Geophysics, Geosystems 13, Q03013.

Pérez-Mejías, C., Moreno, A., Sancho, C., Bartolomé, M., Stoll, H., Osácar, C., Cacho, I., Delgado-Huertas, A., 2018. Geochimica et Cosmochimica Acta 243, 66-98.

Pflitsch, A., Wiles, M., Horrocks, R., Piasecki, J., Ringeis, J., 2010. Dynamic climatologic processes of barometric cave systems using the example of Jewel Cave and Wind Cave in South Dakota, USA. Acta Carsologica 39, 449-462.

Plata, A., 1994. Composición isotópica de las precipitaciones y aguas subterráneas de la Península Ibérica. CEDEX, Madrid.

Thornthwaite, C.W., 1948. An approach toward a rational classification of climate. Geographical Review 38, 55-94.

Treble, P.C., Bradley, C., Wood, A., Baker, A., Jex, C.N., Fairchild, I.J., Gagan, M.K., Cowley, J., Azcurra, C., 2013. An isotopic modelling study of flow paths and storage in Quaternary calcarenite, SW Australia: implications for speleothem paleoclimate records. Quaternary Science Reviews 64, 90-103.

Villar, E., Fernandez, P.L., Quindós, L.S., Solana, J.R., Soto, J., 1983. Temperature of rock surface in Altamira Cave (Spain). Transactions of the British Cave Research Association 10, 165-170.

Wackerbarth, A., Scholz, D., Mangini, A., 2010. Modelling the $\delta^{18}O$ value of cave drip water and speleothem calcite. Earth and Planetary Science Letters 299, 387-397.

Wang, Y.D., Cheng, H., Edwards, R.L., An, Z.S., Wu, J.Y., Shen, C.C., Dorale, J.A., 2001. A high-resolution absolute-dated Late Pleistocene monsoon record from Hulu Cave, China. Science 294, 2345-2348.

Yamada, M., Ohsawa, S., Matsuoka, H., Watanabe, Y., Brahmantyo, B., Maryunani, K.A., Tagami, T., Kitaoka, K., Takemura, K., Yoden, S., 2008. Derivation of travel time of limestone cave drip water using tritium/helium 3 dating method. Geophysical Research Letters, 35, L08405.

Yonge, C.J., Ford, D.C., Gray, J., Schwarcz, H.P., 1985. Stable isotope studies of cave seepage water. Chemical Geology 58, 97-105.

FIGURE CAPTIONS

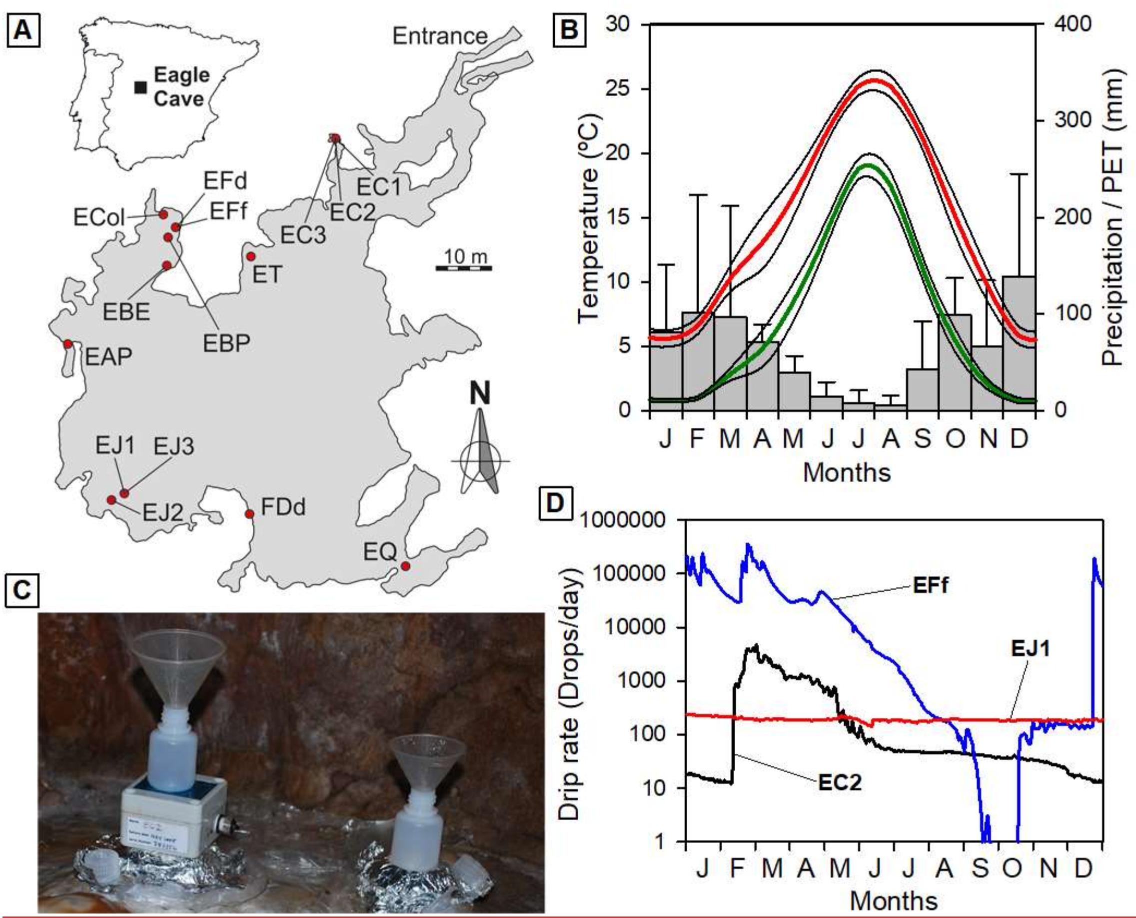

Fig. 1. Eagle Cave settings and sampling sites. A) Sketch of Eagle Cave showing the location of sampling sites. The inset map (top left) shows the cave location within the Iberian Peninsula. B) Climate diagram of the studied site for the years 2009 to 2013, including potential evapotranspiration. Curve in red represents temperature, in green is for PET and grey bars are for precipitation. C) Drip sites EC1 (left) and EC2 (right) during a water collection campaign. D) Examples of annual drip rate records from 3 drip sites with different flow regimes. EFf: highly variable drip rate and discontinuous flow, EJ1: limited drip rate and continuous flow, EC2: bi-modal drip rate and continuous flow.

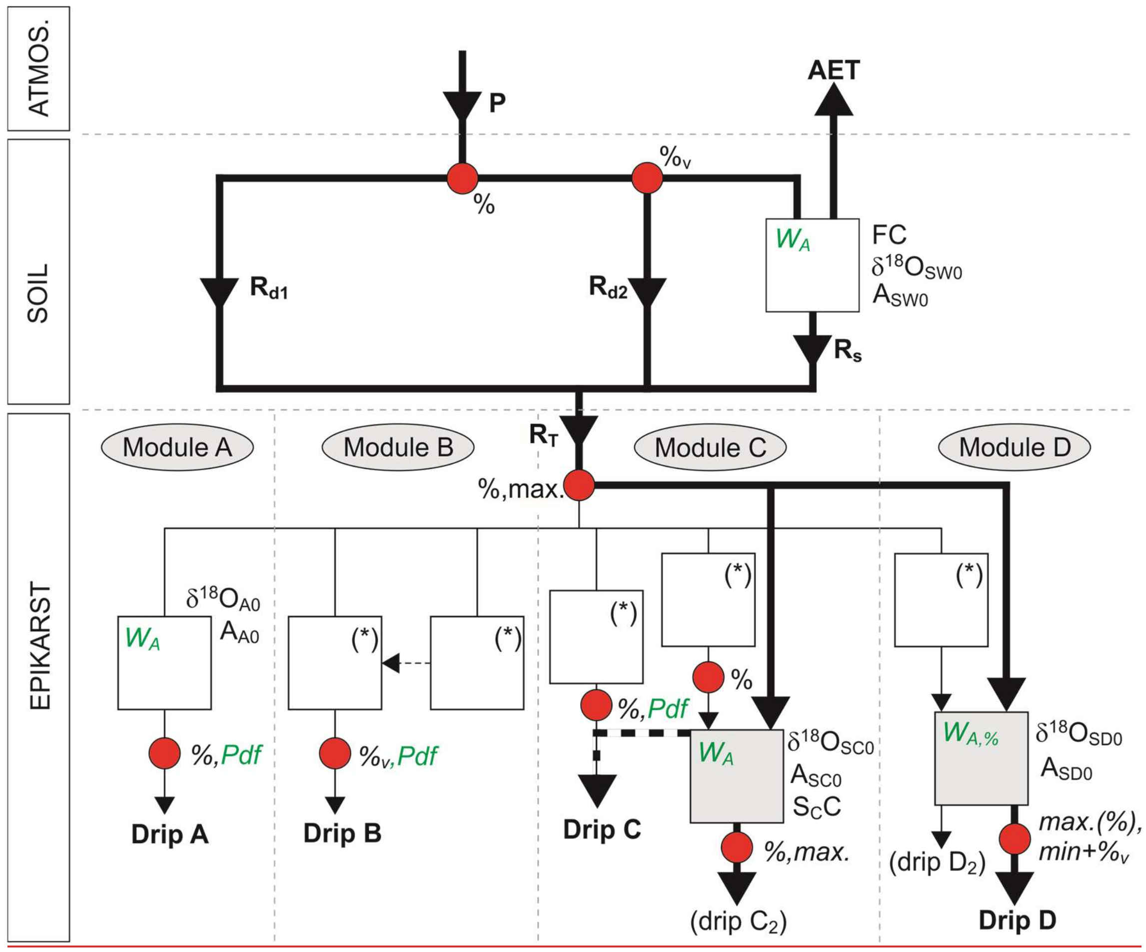

Fig. 2. Sketch of ISODRIP model to simulate the isotope composition of vadose zonewaters. The model has three layers, atmosphere, soil and vadose zone and four modules to represent different hydrological scenarios in the vadose zone layer. Module A is for diffuse drainage under atmospheric pressure, module B for diffuse flow under temporal overpressure conditions, module C is for drainages with preferential and diffusional flows circulating through an overflow storage that results in continuous discharge and module D for drainages with preferential and diffuse flows circulating through an underflow storage that results in discontinuous discharge. The output of the model provides the amount of water and the isotope composition of different drips in a hypothetical cave. Lines and arrows indicate the flow of water in the system as

preferential flow drainage (thick lines) or diffuse flow drainage (thin lines). Discontinuous lines represent conditional flow. Rectangles represent water reservoirs, they have a white filling when the reservoir is a network across the full layer (i.e., soil interconnected porosity and vadose zone diffuse flow network) or are filled in grey color when they represent storages (i.e., large open fissures or other cavities) within the vadose zone. The isotope composition of water in every reservoir is averaged considering the amount of water from each contributing source. W_A: Isotope values weighted by the amount of water from every contributing source, including the reservoir itself. Red dots are nodes where the flow is controlled by at least one operation. All operation symbols are in italics, colored in green when describing just a function, or in black when the function requires entering an input parameter to be defined by the user. $W_{A,\%}$: Isotope values calculated using a percentage for every source of water in addition to their amount of water contributed. The black % symbol indicates that a percentage of water can flow in a certain direction, the rest being directed in a different direction or continues being accumulated in the preceding reservoir. $\%_v$: indicates that the percentage of flow is variable. Pdf is a probability distribution function. max. and min.: are maximum or minimum thresholds of flow; max. (%): a maximum percentage of flow is considered. Drip A, B, C and D are the main drips simulated, although the model also includes two subsidiary outflows or drips (i.e., drip C_2 and D_2) that are only introduced to keep the mass balance. Initial amount of water (A_0) and isotope composition (δ_0) of different reservoirs are required input parameters. These reservoirs are indicated by the subscripts: SW for the water accumulated in the soil, A for water in the diffuse flow network, SC and SD for water in the storages from module C and D, respectively. Other variables are also reported in this sketch. P stands for precipitation, AET is the actual evapotranspiration; R_{d1} and R_{d2} are two components of direct recharge, R_T is the total recharge and FC the field capacity. In module C, the storage that collects preferential flows has a maximum capacity (CS_C) controlled by the position of the overflow conduit. The symbol (*) in epikarst reservoirs indicates that the initial parameters and average weighting in these reservoirs is identical to the reservoir in the module A.

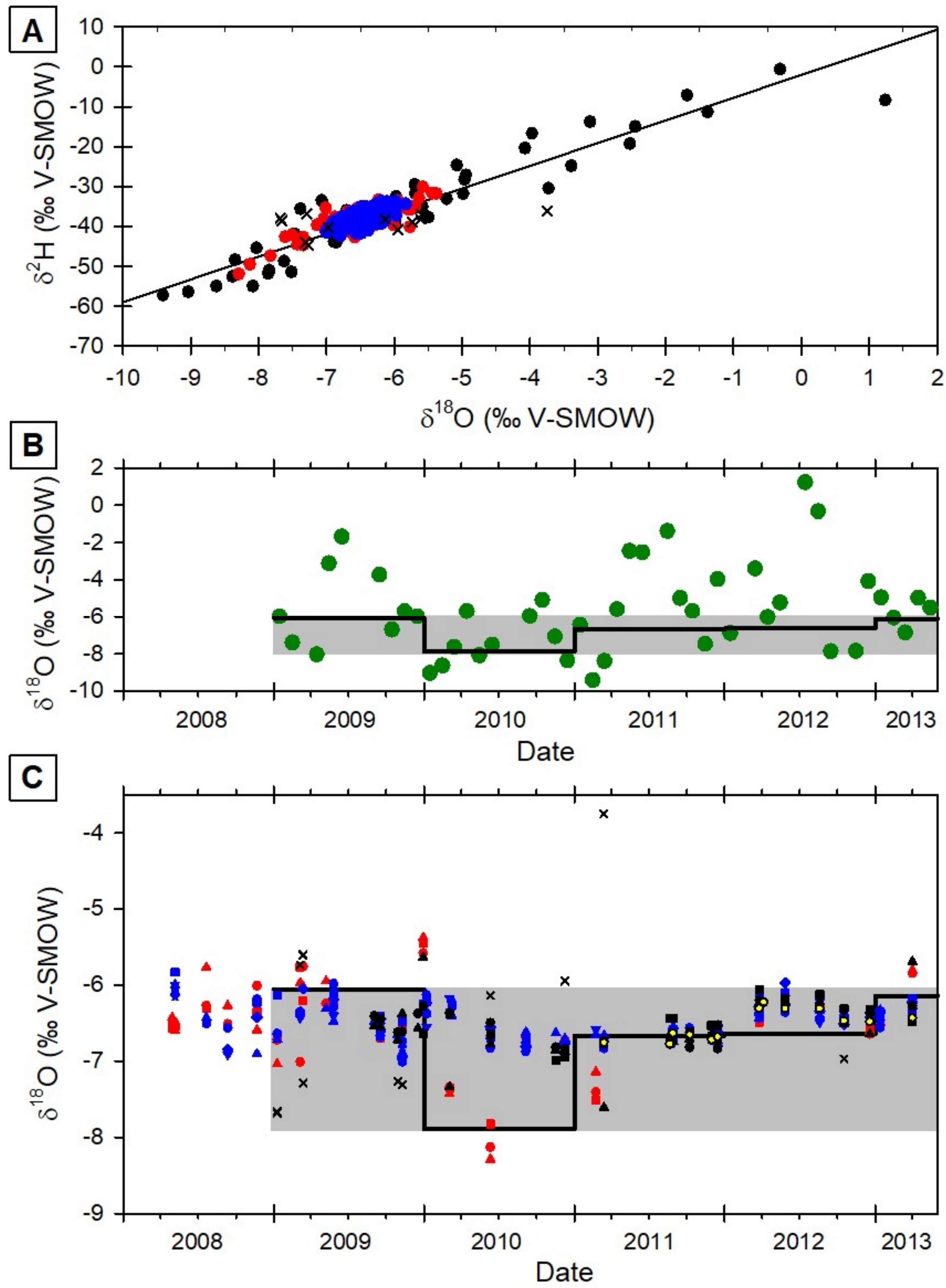

Fig. 3. Isotope records at the studied site. A) Graph showing the δ^2H and $\delta^{18}O$ relationship of precipitation and cave waters. Black dots: monthly rainwater samples. Red dots:

partially-mixed cave waters. Blue dots: well-mixed cave waters. Crosses: anomalous analyses. Cave waters overlie the local meteoric water line with no signs of deviation due to evaporation. B) Monthly precipitation δ^{18}O record (green dots) at the meteorological station outside Eagle Cave. The black line shows the annually weighted δ^{18}O record of precipitation ($\delta^{18}O_{pw}$). The grey rectangle shows the range of variability of $\delta^{18}O_{pw}$. C) Cave water δ^{18}O record. The black line and grey rectangle are the $\delta^{18}O_{pw}$ record as in the panel B. Red symbols: drip sites with partially-mixed waters (triangle: ECol, circle: Eff, square: EFd). Blue symbols: drip sites with well-mixed waters (star: EBE, triangle: ET, circle: EJ1, square: EJ3, diamond: EJ2, hexagon: EC1, inverted triangle: EC2, vertical stripe: EC3). Black symbols: Pool waters (triangle: EBP, circle: EAP, square: FdD), Yellow circles: water equilibrated with the cave atmosphere. Crosses: anomalous analyses.

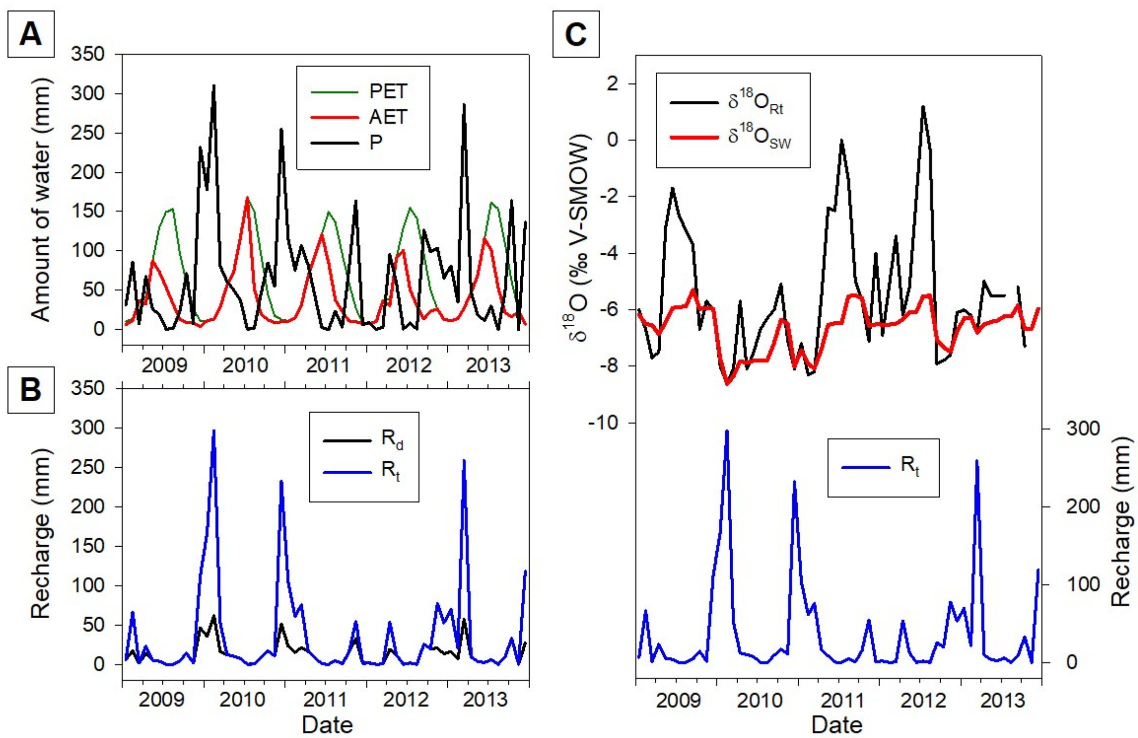

Fig. 4. Simulation of time series of the soil water components and their isotope composition above Eagle Cave during the period 2009-2013. A) Graph showing the relationship among precipitation (P), potential evapotranspiration (PET) and actual evapotranspiration (AET). B) Main contributions to recharge. The direct recharge (R_d) represents the sum of the two direct recharge components considered in ISODRIP, R_{d1} and R_{d2}. Total recharge (R_T) is the sum of soil recharge (R_S) and direct recharge (R_d) components. C) Isotope composition of water stored in the soil (red curve) and total recharge water (black curve). The lower panel shows the amount of recharge every month. Outstanding positive/less negative isotope anomalies of water from the R_d source contributes to the recharge with small but significant amount of water. Large peaks of R_T (blue curve) occur during different periods of the year and during those periods, the isotope variability range of R_T (black curve) is < 2‰.

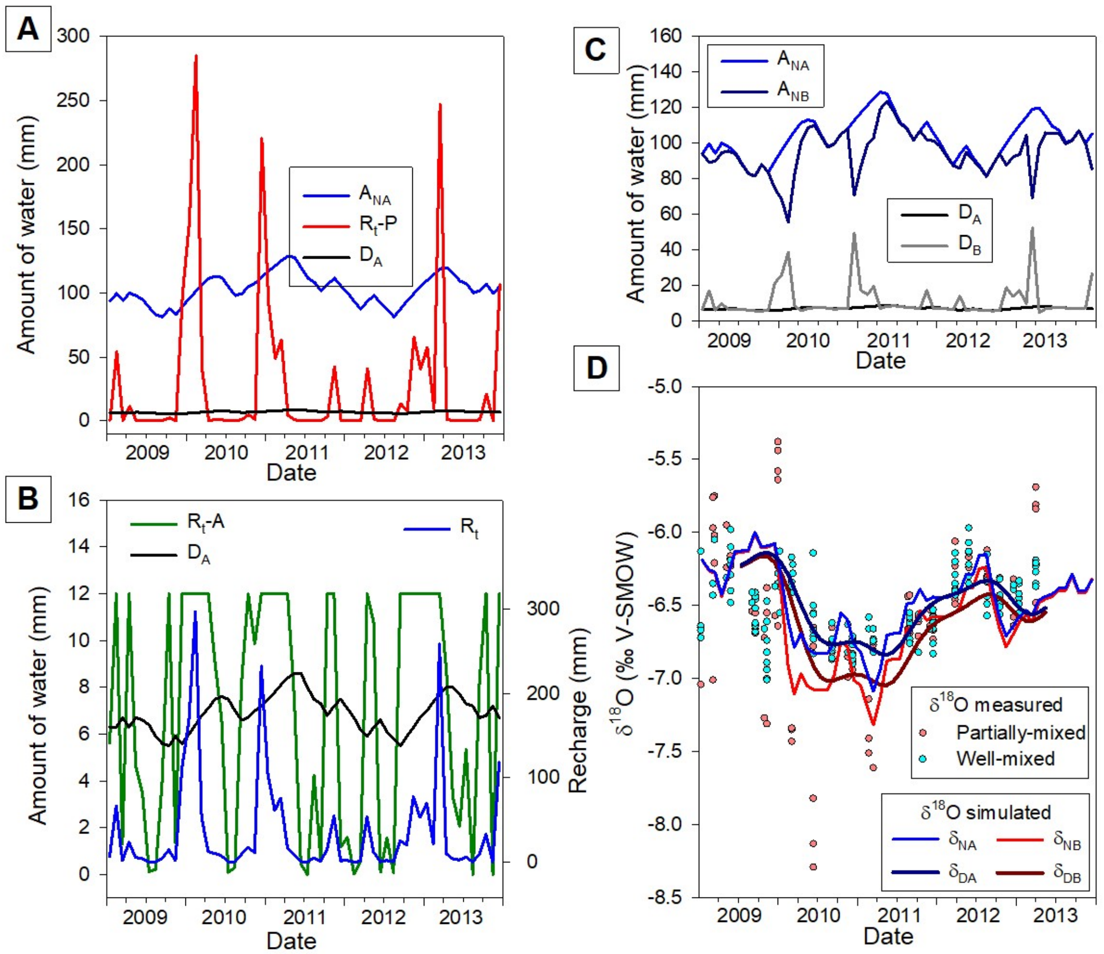

Fig. 5. Simulation of diffuse flow drainage in modules A and B. A) Main hydrological components of module A simulation. A_{DfA}: amount of water accumulated in the diffuse flow network of module A, R_{TPf}: amount of total recharge diverted to preferential flows, Q_A: discharge at drip site A. B) Details of the hydrological response of module A. R_T: total recharge, R_{TDf}: amount of total recharge that enters the diffuse flow network. The right axis is scale only for R_T. C) Main hydrological components of modules A and B.

Amount of water accumulated in the diffusional flow network of modules A and B (A_{DfA} and A_{DfB}). Discharge at drip sites A and B (Q_A and Q_B). D) Simulated $\delta^{18}O$ signal of water from the upper section of the aquifer according to modules A and B (δ_{DfA} and δ_{DfB}) and at the drip sites A and B (δ_A and δ_B). Observed $\delta^{18}O$ data are also plotted for comparison.

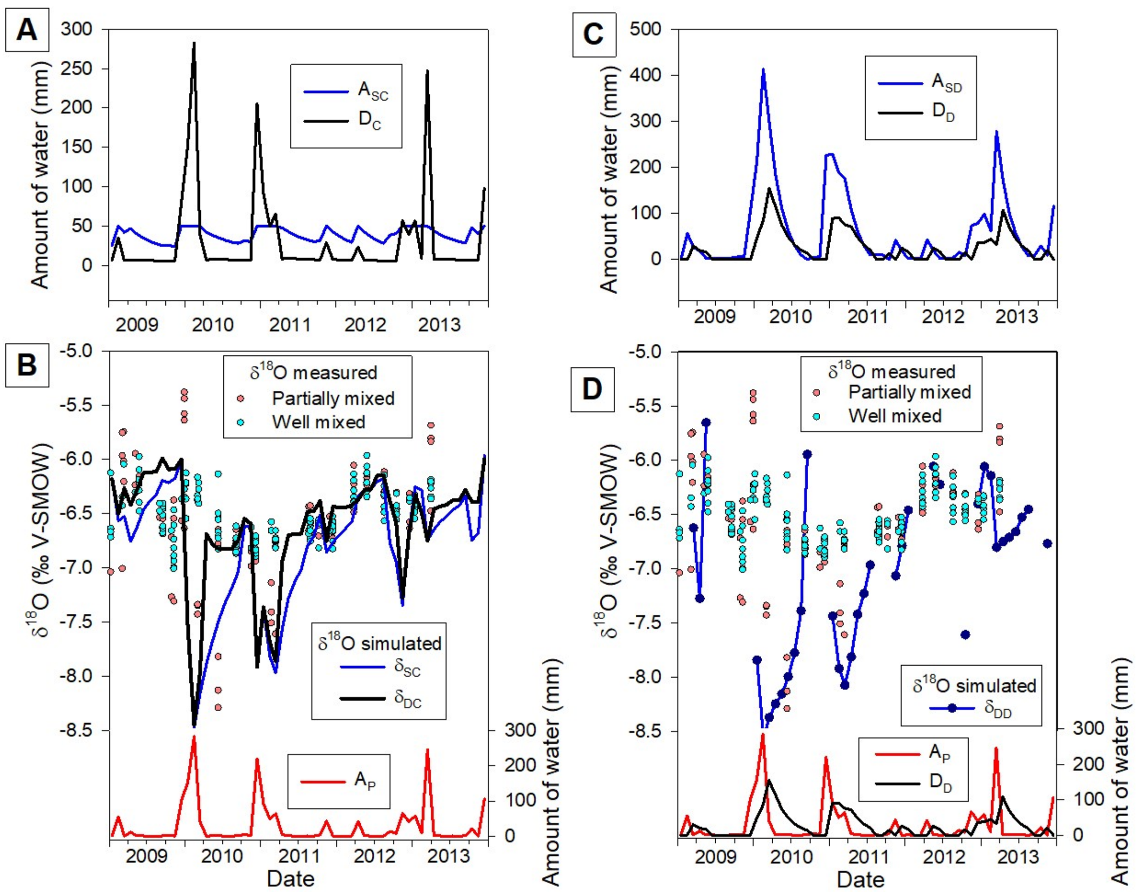

Fig. 6. Simulations of drainages with preferential flow components in modules C and D. A) Main hydrological components of preferential flow in module C. A_{SC}: amount of water in the storage of module C, Q_C: discharge at drip site C. B) Simulated $\delta^{18}O$ signal of water in the storage C (δ_{SC}) and at the drip site C (δ_C). Observed $\delta^{18}O$ data are plotted for comparison. The amount of water provided by preferential flows (R_{TPf}) is plotted for

comparison. C) Main hydrological components in module D. A_{SD}: amount of water in the storage of module D, Q_D: discharge at drip site D. D) Simulated $\delta^{18}O$ signal of water at the drip site D (δ_D). Observed $\delta^{18}O$ data are also plotted for comparison. The amount of water provided by preferential flows (R_{TPf}) and the discharge of drip D (Q_D) are plotted for comparison.

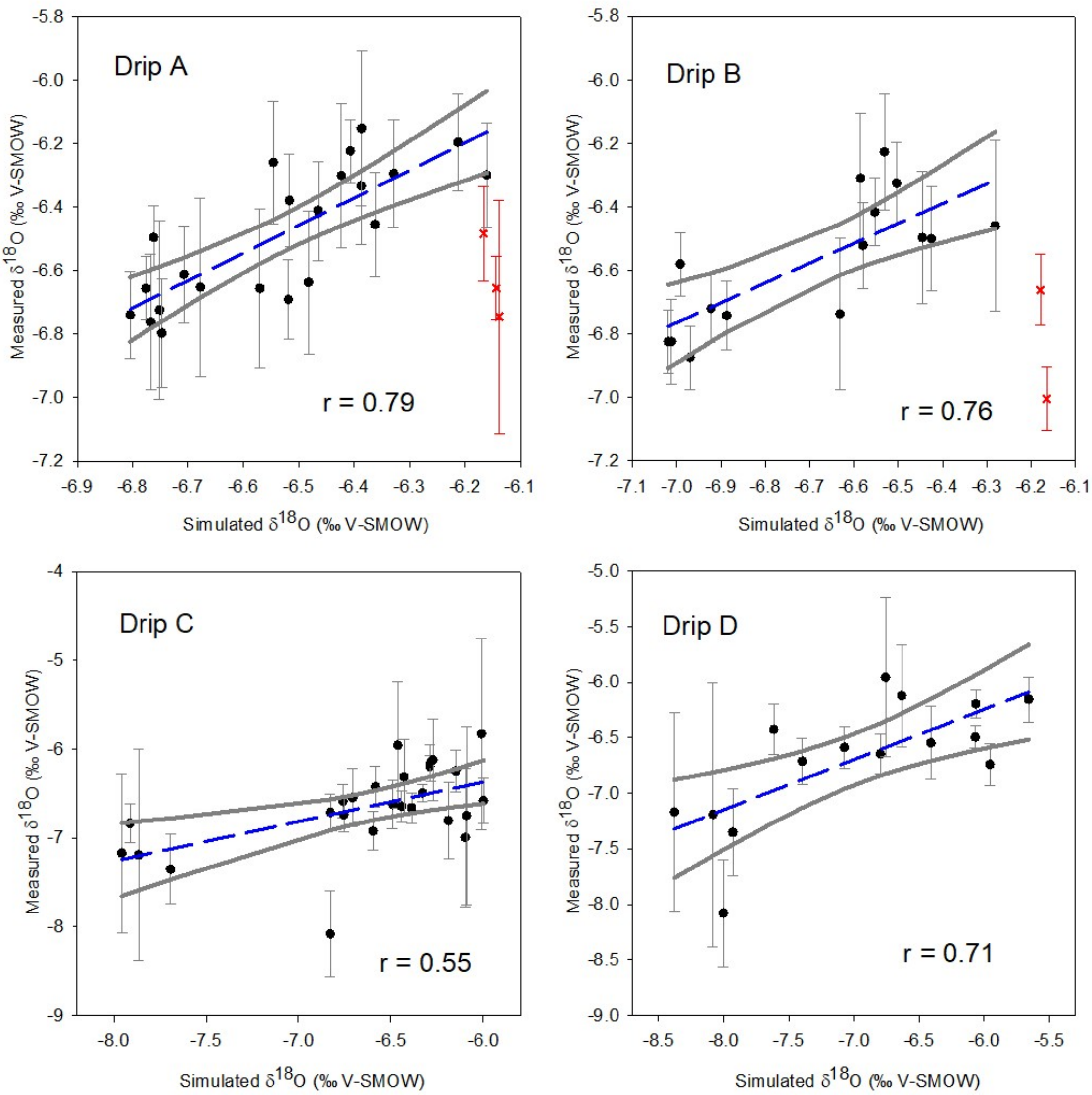

Fig. 7. Comparison of simulated $\delta^{18}O$ signals of drips from modules A, B, C, and D with observed $\delta^{18}O$ records from sites classified into the four hydrological modules of ISODRIP. All partially-mixed waters were used to compare the simulations of drips C and D, although only those months with simulated discharge in drip D were used for comparison in the case of module D. For every month, observations of all drips characterized for a particular module were averaged. The vertical uncertainty bars accounts for two standard deviations of all observations for sites within each module and sampling campaign as well as the analytical error. The regression (blue dashed line) and the 95% confidence interval bands (grey lines) of the model-observation correlation are also plotted to evaluate the overlap of uncertainties. Clear outlier data from drips A and B (red crosses with their error bars) were removed from calculations (see supplementary material).

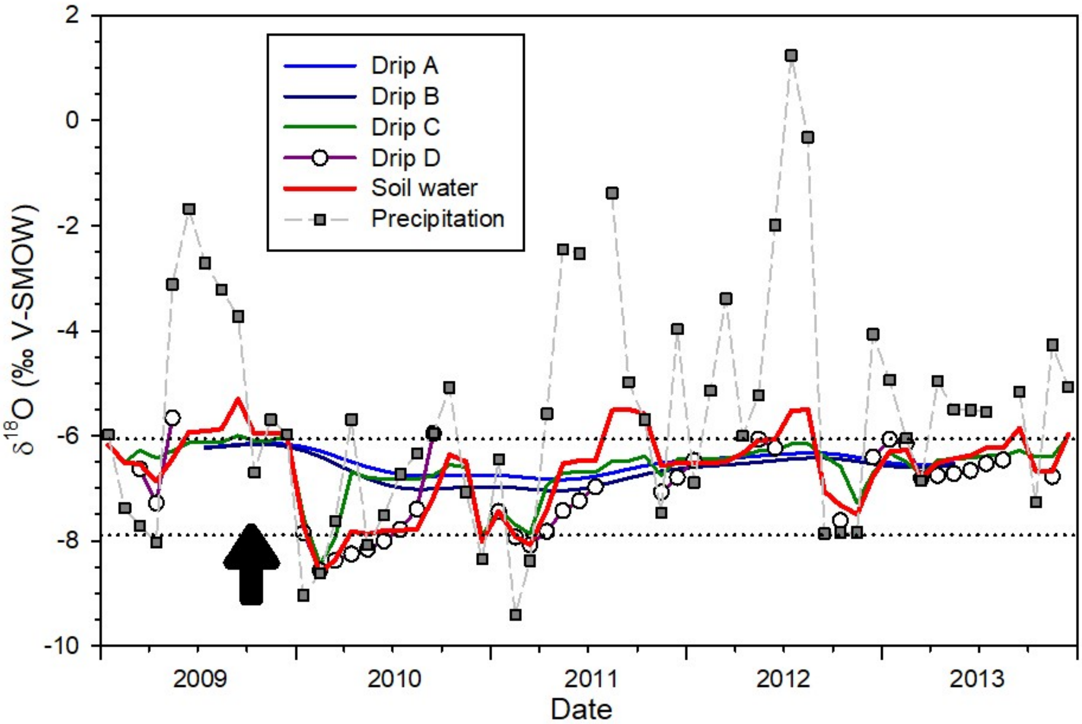

Fig. 8. Drip and soil water $\delta^{18}O$ simulations. Monthly precipitation $\delta^{18}O$ record is displayed for comparison. Dotted horizontal lines represent the range of annually weighted $\delta^{18}O$ values of precipitation. The black arrow indicates the period that cause outliers in simulated drips A and B.